

## PLS 2 GeV Linac Vacuum System (II)

J. S. Bak, Y. K. Kim, H. S. Oh\* and W. Namkung

Linac Division, Pohang Accelerator Laboratory, POSTECH  
P.O. Box 125, Pohang 790-600, Korea

\*Research and Development Center, POSCON, Pohang 790-380, Korea

(Received July 28, 1993)

## PLS 2 GeV 線形加速器 眞空系統 (II)

박주식 · 김임경 · 오형석\* · 남궁원

포항가속기연구소 선형가속기개발단

\*(주) 포스콘기술연구소

(1993년 7월 28일 접수)

**Abstract** — The vacuum system of the PLS 2 GeV linac has been assembled and installed successfully up to the K6 module. Two regular linac modules (K2 and K3) have been already conditioned with 70 MW microwave power from E3712 klystron. Now, the pressures range from  $6.2 \times 10^{-8}$  torr at the accelerating column center (L-type), to  $7.3 \times 10^{-8}$  torr at the klystron window with about 50 MW microwave power loading, and the ultimate pressures will become progressively lower. This presentation describes the electrical modeling and analysis, and the initial performances for the first half of the PLS 2 GeV linac vacuum system.

**요 약** — PLS 2 GeV 線形加速器的 眞空系는 K6 가속단위까지 성공적으로 조립, 설치되어 있다. K3 가속單位까지는 이미 E3712형 클라이스트론에서 공급되는 70 MW 極超短波 電力으로 진공계 길들이기 과정을 완료하였다. 약 50 MW의 극초단파 전력을 인가한 상태에서, 현재 진공도는 L-형 가속管 中心에서  $6.2 \times 10^{-8}$  torr, 클라이스트론 出力窓에서  $7.3 \times 10^{-8}$  torr를 각각 유지하고 있으며, 最終 到達壓力은 點差의으로 向上되고 있는 중이다. 본 논문에서는 PLS 2 GeV 線形加速器 眞空系에 대한 電氣回路的 變換에 의한 모델링과 解析, 그리고 加速器 前半部에 關한 初期 性能 檢證結果를 論議하고자 한다.

### 1. Introduction

PAL(Pohang Accelerator Laboratory) is constructing a 2 GeV electron linac as a full energy injector for the PLS(Pohang Light Source). The third milestone for this linac construction, which is now authorized, is to accelerate the electron beams up to an energy of about 450 MeV by the 60 MeV preinjector unit[1] and two regular linac modules equipped with SLED[2].

The major part of the PLS 2 GeV linac vacuum system consists of 42 OFHC brazed accelerating columns and about 400 m long rectangular wave-

guides. Presently, the PLS 2 GeV linac vacuum system, which was completed up to the K6 module, is providing a base pressure in the low  $10^{-8}$  torr range under the condition of about 50 MW microwave power transmission. In this paper we will summarize the results of our experiments on (1) electrical modeling and analysis, (2) outgassing measurement, (3) vacuum behaviour during the RF processing, and (4) leak detections.

### 2. System Description

The 150 m long PLS 2 GeV linac consists of 10

nearly identical 14 m long modules and a 60 MeV preinjector unit. Each module contains four 3.072 m long accelerating columns composed of a string of 86 S-band cavities, five connecting bellows and some cylindrical stainless steel construction components. The RF power of up to 80 MW over 4  $\mu$ sec from each E3712 klystron located in a gallery above the linac tunnel is fed to four travelling wave accelerating structures via about 40 m of evacuated  $72 \times 34$  mm rectangular waveguides. All metal sector valves mounted in the intersector are used to isolate four vacuum sectors. The preinjector with associated equipments (electron gun, prebuncher and buncher) is isolated with valve and formed specific subsystems.

Each module is pumped down by four 60 l/sec triode sputter ion pumps in tunnel and two 120 l/sec ion pumps (Starcell, trademark by Varian) in gallery for UHV pumping, and by two 220 l/sec turbomolecular pump units for initial start-up. Pressure measurements for each module are also achieved by two cold cathode gauges and two BA gauges [3].

The large number of individual vacuum components are related to the scale of the PLS 2 GeV linac. More than 1300 construction components are required for 10 modules assembling. More than 60 sputter ion pumps, 12 isolation gate valves, 20 BA ionization gauges and more than 20 penning discharge gauges will have to be permanently powered and monitored. The vacuum control system is separately integrated into three local stations in gallery.

### 3. Electrical Modeling and Analysis

The analysis of a large and complex vacuum system such as the PLS 2 GeV linac is a very tedious process, especially when distributed loads and

pumps are involved. It has been suggested that a complicated vacuum system can be modeled as an electrical circuit by using the appropriate transformations[4, 5]. The correspondences between vacuum metrics and electrical metrics are summarized in Table 1. Here we attempted to model the regular linac vacuum module into the electrical network. Fig.1 shows the electrical representation of the K4 vacuum module. Each accelerating column composed of a string of 86 S-band copper cavities is divided into six segments. The outgas loading on each vacuum element is obtained from the outgassing rate to be described in next section. To preserve the accuracy of the circuit analysis code, a scaling factor of  $1 \times 10^6$  is applied to the gas loads. Unless source scaling is properly used, the matrix equations used in the analysis code are often unstable, or difficult to solve accurately. Each ion pump is modeled as the series combination of a resistive element and a constant voltage source. The ultimate pressure of the ion pump, which is described as voltage across the constant voltage source in Fig. 1, is assumed to be  $1 \times 10^{-10}$  torr. The circuit analysis code used for this analysis is P-SPICE, which runs on PC compatible computers. Basic parameters needed for this analysis are listed in Table 2. The steady state (outgassing only) vacuum profiles analyzed by the P-SPICE code are shown in Fig. 2. The horizontal axes represent dis-

**Table 2.** Basic parameters of a typical vacuum module

System component	Conductance $S, (l/s)$	Outgassing $I_{out} (torr \cdot l/s)$	Volume $V, (l)$
Accelerating column	0.5	$4.7 \times 10^{-7}$	14.4
Waveguide/3 m long	6.7	$1.9 \times 10^{-7}$	7.4
Energy doubler	40	$2.2 \times 10^{-6}$	30
Dummy load	20	$1.0 \times 10^{-6}$	2.6

**Table 1.** Correspondences between vacuum metrics and electrical metrics

Vacuum metric	Vacuum symbol	Vacuum units	Electrical metric	Electrical symbol	Electrical units
Pressure	<b>P</b>	torr	Potential	<b>E</b>	V
Gas flow	<b>Q</b>	torr·l/sec	Current	<b>I</b>	A
Conductance	<b>S</b>	l/sec	Conductance	<b>Y</b>	mho
Volume	<b>V</b>	l	Capacitance	<b>C</b>	F
Flow controller	<b>K</b>	sec/l	Inductance	<b>L</b>	H

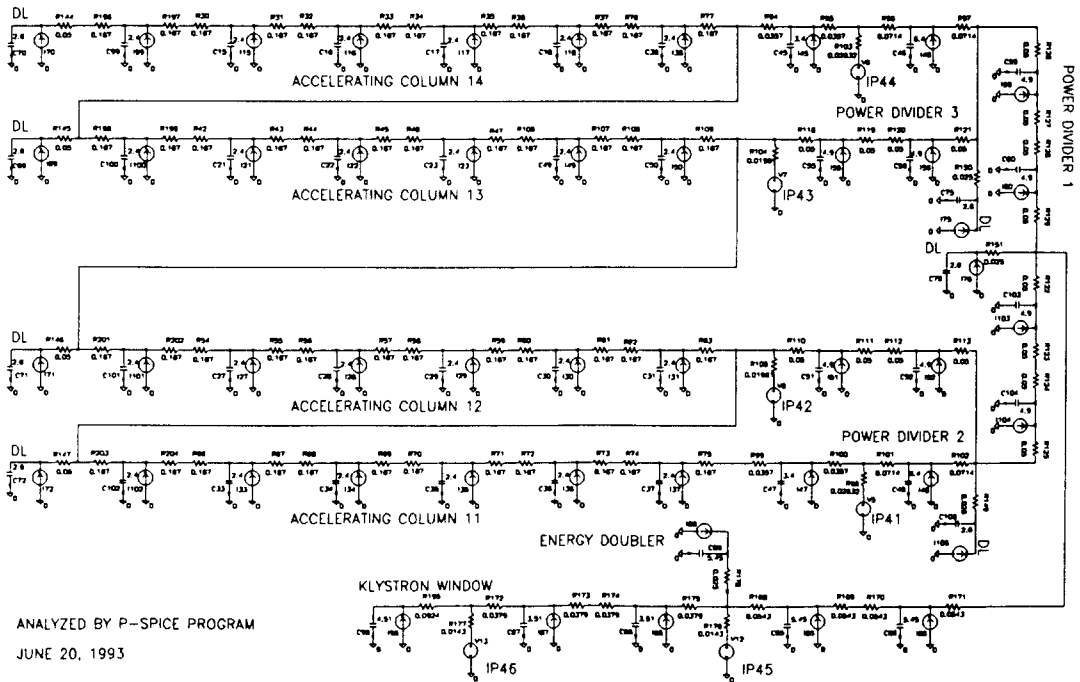


Fig. 1. Electrical representation of the K4 vacuum module.

tance down the electron beam line and the microwave power line in meters, respectively. The vacuum profiles analyzed by the electrical modeling are in good agreement with the data measured by cold cathode gauges and the results calculated by FEM method[6]. The vacuum states shown in Fig. 2 are relatively high in comparison with the preinjector vacuum, which keep up the range of low  $10^{-9}$  torr. That is because its analyses and measurements were done at the infant stage. Presently, the vacuum profiles keep on improving by continuous  $45^{\circ}\text{C}$  bakeout and high power RF conditioning. From these analysis results, we confirmed that the intervals between pumps were optimized. The use of this technique is expected to significantly reduce the effort required to analyze the large scale vacuum system.

## 4. Initial Performances

### 4.1. Outgassing Measurement

Generally, the estimation of outgas loading in a complicated vacuum system is not so easy, because it is very dependent on temperature and environ-

mental history. Here an experiment was made to determine the outgassing rate from a regular module of the PLS 2 GeV linac vacuum by using the rate-of-rise method[7].

For a regular linac module with the inner surface area of about  $42\text{ m}^2$  and the volume of  $0.18\text{ m}^3$ , we obtained the pressure rise curve shown in Fig. 3. This measurement was performed after an uninterrupted bakeout of two weeks at  $45^{\circ}\text{C}$  with continuous pumping. The outgassing rate is calculated to be approximately  $3 \times 10^{-11}\text{ torr}\cdot\text{l}/\text{sec}\cdot\text{cm}^2$  from the pressure difference value taken in Fig. 3. This outgassing rate is three times higher than that of the BEPC (Beijing Electron Positron Collider) injector linac[8, 9]. It is conjectured that the high outgassing rate of  $3 \times 10^{-11}\text{ torr}\cdot\text{l}/\text{sec}\cdot\text{cm}^2$  is due to the no RF aging and long-term storage effects. The gradual RF processing and steady pumping make it possible to reduce the outgassing rate remarkably. Actually, the effective outgassing rate of  $6 \times 10^{-12}\text{ torr}\cdot\text{l}/\text{sec}\cdot\text{cm}^2$  is achieved in the K3 module after two months RF aging. And, it is also confirmed that the main components of released gases are hydrogen, carbon monoxide, and molecules of

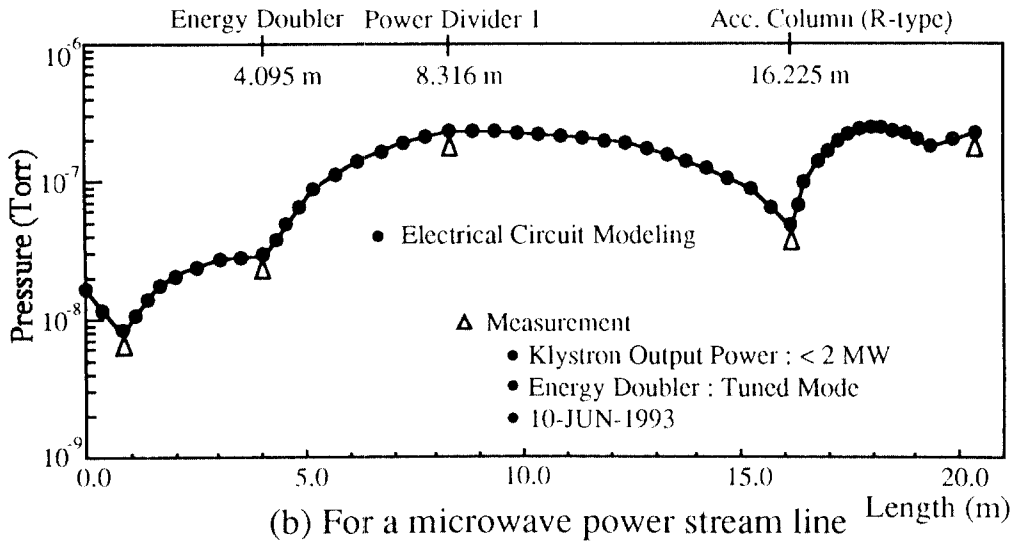
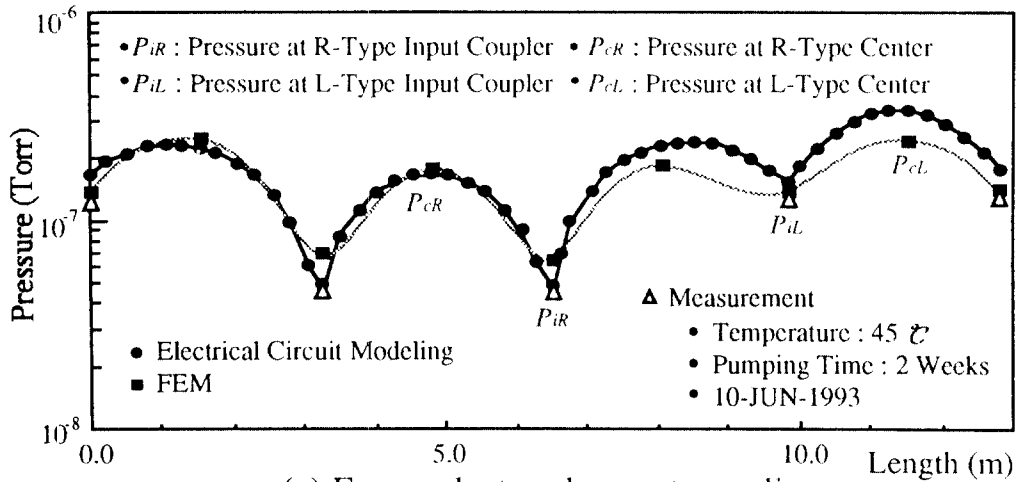


Fig. 2. Vacuum profiles for a regular module.

water vapours.

**4.2. Vacuum Behaviour during RF Processing**

At present, the microwave power conditioning for the first three modules is going on. Fig.4 shows the vacuum history of the K3 module during the RF processing carried out at the power level of 2 MW. As shown in the figure, the resulting RF processing is accompanied by steady outgassing at pressures between  $10^{-8}$  and  $10^{-7}$  torr and interrupted occasionally by a RF breakdown within a few minutes. These breakdown events are explained by

the combination of the following two theories; Explosive Electron Emission(EEE)[10-14] and Field Induced Hot Electron Emission(FIHEE)[15-18]. The pattern of breakdown, subsequent recovery and gradually increasing field continues all the way up to 70 MW klystron output power. From the K2 and K3 module conditioning results, it has taken more than 2 months.

During the microwave power conditioning with 2 MW at 10 Hz, the transient pressure change at the klystron window is shown in Fig.5, which is measured by using the DSA 602A digitizing signal

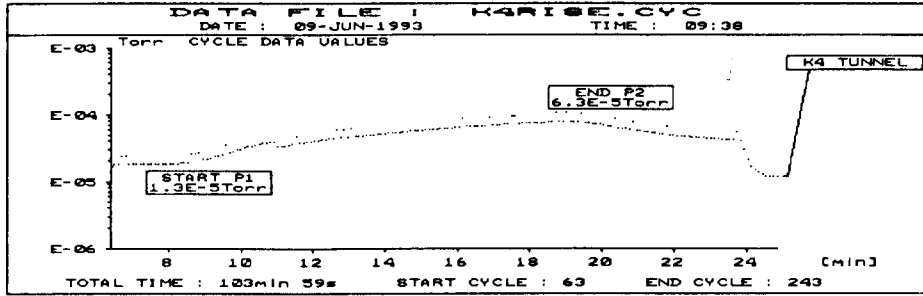


Fig. 3. Pressure rise curve in the K4 module.

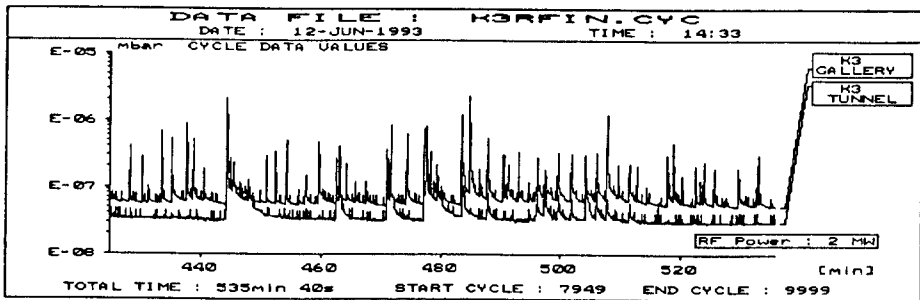


Fig. 4. Vacuum history during K3 module RF processing.

analyzer. The horizontal axis represents response time, in 100 msec/div. The 2856 MHz microwave power is fed into the vacuum system for 4 μsec macropulse period every 100 msec. When the pressure exceeds the interlocking level of  $4 \times 10^{-7}$  torr, the triggering for the klystron modulator should be immediately stopped. But, the trigger signal for next output pulse is not inhibited. It is presumed that this delayed action is caused by inherent vacuum feature and/or vacuum gauge controller[19]. The faster response for pressure change is required to operate the modulator with higher pulse repetition rate.

4.3. Leak Detections

188 ConFlat-type and 312 Skarpaas-type flange pairs were installed in the first 5 modules (K2-K6). In the first stage of assembly work, 89% of the total joints were leak free to less than  $1.5 \times 10^{-10}$  torr·l/sec. Most leaks were mainly originated from the following defects; material, mounting, machining tolerances, and cleaning. Several leaking flange pairs were scratched and nicked. Flanges with too

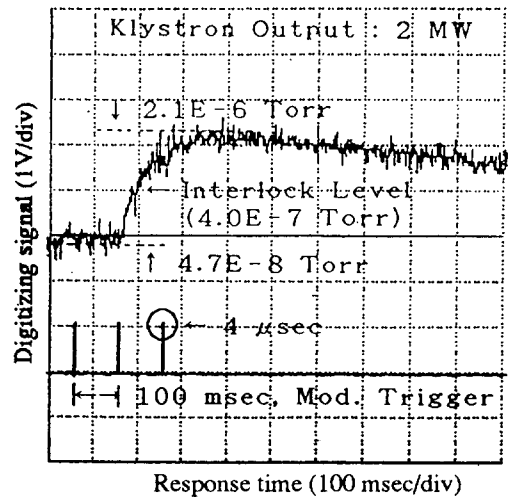


Fig. 5. Relationship between modulator triggering and vacuum behaviour the K3 module conditioning.

shallow gasket grooves or flange pairs with different knife-edge diameters or profile shapes sometimes made umbréllalike gasket deformations. These deformations caused the reduction of the elastic gasket compression and the loss of the sealing fo-

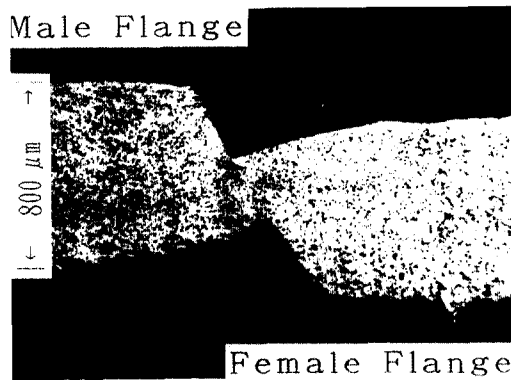


Fig. 6. Deformation of the waveguide gasket after use.

rice. Some of leaking gaskets were found with imprints of fibers or small chips. Besides, on several occasions leaks were detected on the brazed joints between SUS 304 W/G flange and rectangular copper tube. These leaks were due to the misplacement of the braze alloy and careless cleaning of the components. We also found that the tightly adherent oxide thin films on the flange or gasket surface didn't give any leakage effects. Fig. 6 is a picture of the deformed waveguide gasket (Skarpas type)[20], which was made of the annealed OFHC copper. Its thickness and Vickers hardness were 0.8 mm and 67, respectively. The roughness of machined surface was in the range of 0.1~1.0  $\mu\text{m}$ . The critical alignment of the W/G gaskets during assembly was achieved by a special clamping tool with two precision dowels.

## 5. Conclusions

We achieved the base pressures of the low  $10^{-8}$  torr range and the medium  $10^{-9}$  torr range, with and without *in situ* bakeout of 45°C and RF power transmission, respectively. These pressure ranges will ideally suit for building up the high accelerating gradient of above 20 MV/m. Meanwhile, more work is required to explain the interesting vacuum phenomena during the RF processing.

It is definitely affirmed that the *in situ* assembling of a large machine such as the PLS 2 GeV linac can easily suffer from fiber contaminations, bad accessibility for the assembly work and tolerance faults. Therefore, these three factors determine

the limit of reliability of the PLS 2 GeV linac vacuum system.

## Acknowledgements

This research was supported by the Pohang Iron and Steel Co. and the Ministry of Science and Technology, Korea.

## References

1. W. Namkung *et al.*, Proceedings of the Third European Particle Accelerator Conference, Vol I, 507 (1992).
2. W. Namkung *et al.*, Proceedings of the Third KAPRA Workshop (1993).
3. 김임경, 오형식, 이인준, 박주식, 남궁원, 한국진공학회지 **2**, 17 (1993).
4. S. Dushman, *Scientific Foundations of Vacuum Technique* (Wiley, New York, 1949).
5. B. R. F. Kendall, *J. Vac. Sci. Technol.* **A1**, 84 (1983).
6. *Design Report of Pohang Light Source*, Revised ed. (Pohang Accelerator Laboratory, POSTECH, 1992).
7. Varian's Vacuum Products Division, *Basic Vacuum Practice*, 2nd ed. (Varian Associate Inc., Palo Alto, 1989).
8. BEPC Design Gr., *Preliminary Design of Beijing 2.2 /2.8 GeV Electron Positron Collider* (IHEP, Beijing, 1982).
9. S. Zhou, *Particle Accelerators*, **27**, 113 (1990).
10. R. V. Latham, *High Voltage Vacuum Insulation* (Academic Press, New York, 1981).
11. C. S. Watters, M. W. Fox and R. V. Latham, *J. Phys. D: Appl. Phys.* **7**, 911 (1974).
12. G. A. Farrall, M. Owens and F. C. Hudda, *J. Appl. Phys.* **46**, 610 (1975).
13. B. M. Cox, *J. Phys. D: Appl. Phys.* **8**, 2065 (1975).
14. G. A. Mesyats, *IEEE Trans. Elect. Insul.* **EI-18**, 218 (1983).
15. T. S. Sudarshan, J. D. Cross and K. D. Srivastava, *IEEE Trans. Elect. Insul.* **EI-12**, 200 (1977).
16. C. S. Athwal, R. V. Latham, *Physica* **104C**, 189 (1981).
17. R. V. Latham, *Vacuum* **32**, 137 (1982).
18. R. V. Latham, *Proceedings XIIIth Int. Symp. on Discharges and Electrical Insulation in Vacuum* (1986).
19. *Operating Instructions for Total Pressure Gauge and Controller*, 3rd ed. (Balzers, Liechtenstein, 1988).
20. R. B. Neal, ed., *The Stanford Two-Mile Accelerator*, (Benjamin Inc., New York, 1968).